Electrodes from carbon nanotubes/NiO nanocomposites synthesized in modified Watts bath for supercapacitors

AUTHOR(S):

Hakamada, Masataka; Abe, Tatsuhiko; Mabuchi, Mamoru

Electrodes from carbon nanotubes/NiO nanocomposites synthesized in modified Watts bath for supercapacitors

Masataka Hakamada*, Tatsuhiko Abe, Mamoru Mabuchi

Department of Energy Science and Technology, Graduate School of Energy Science, Kyoto University, Yoshidahonmachi, Kyoto, 606-8501 Japan

*Corresponding author. E-mail: hakamada.masataka.3x@kyoto-u.ac.jp (M. Hakamada).

Abstract

A modified Watts bath coupled with pulsed current electroplating is used to uniformly deposit ultrafine nickel oxide particles (diameter < 4 nm) on multiwalled carbon nanotubes. The capacitance of the multiwalled carbon nanotubes/nickel oxide electrodes was as high as 2480 F g^{-1} (per mass of nickel oxide), which is close to the theoretical capacitance of NiO.

Keywords:

Multiwalled carbon nanotubes, nickel oxide, supercapacitor, Watts bath, pulsed current electroplating

1. Introduction

Nickel species such as nickel oxide (NiO) and nickel hydroxide ($Ni(OH)_2$) particles, which show redox reaction and consequent pseudocapacitive behaviour in an electrolyte, are frequently deposited on multiwalled carbon nanotubes (MWCNTs) to obtain a bigger surface area and a uniform dispersion [1–16]. The nanocomposite electrodes of MWCNTs/Ni species (including Ni, NiO and $Ni(OH)_2$) have been effectively fabricated by electroless plating [14–20] electroplating [1,3–5,8,13,21], impregnation [22,23] and other processes [2,9,11].

Pulsed current electroplating, in which the applied potential is oscillated at high frequencies, is another strategy used to fabricate nanostructured Ni [24–26]. Previous studies on pulsed current electroplating of Ni use a Watts bath, which is a conventional electroplating solution for Ni coating. In the present study, we use a modified Watts bath that has a lower concentration of Ni^{2+} than that of a conventional one to reduce the size of the Ni particles deposited on the MWCNTs. The modified bath coupled with pulsed current electroplating can be used to synthesize extraordinarily small (less than 4 nm) Ni oxide species.

2. Experimental

Commercially available MWCNTs (FloTube 9000, prepared by a catalytic vapour deposition process) were provided by CNano Technology Ltd (Santa Clara, CA, USA). The raw CNTs were first treated in a concentrated mixture of 15.6 mol L^{-1} nitric acid and 18.3 mol L^{-1} sulphuric acid (with a volumetric ratio of 1:3) at 333 K for 8 h. The treated CNTs were then washed several times by ultrasonication in distilled water to remove excess acid and then dried in air.

Following the acid treatment, electrophoretic deposition (EPD) was performed to fabricate the CNT film. The negative and positive electrodes were Pt and SUS316L (The Nilaco Corp., Tokyo, Japan) foils with exposed areas of 20–25 mm^2 and a thickness of 20 μm. The distance between the electrodes was 20 mm. The acid-treated CNTs were suspended at a concentration of 0.5 g L^{-1} in distilled water for EPD. A voltage of 30 V was applied between the electrodes at room temperature for 30 s. After EPD, the CNT thin film was dried in air and heated at 673 K for 1 h to oxidize and insulate the SUS316L substrate. This oxidation step facilitated the preferential electrodeposition of Ni on the CNTs rather than on the untreated SUS316L substrate. No loss of CNT due to possible burning in air was observed, which coincides with the high temperature stability of MWCNTs in air [27].

After EPD and oxidation of SUS316L, pulsed current electroplating of Ni was performed on the CNTs to fabricate the CNT/Ni nanocomposite thin film. The pulsed current was a set of +3 A cm^{-2} for 20 μs and −3 A cm^{-2} for 10 μs. This pulsed current was applied for 0.35 s. The electrolyte was composed of $NiSO_4 \cdot 6H_2O$ (24 g L^{-1}), Na_2SO_4 (117 g L^{-1}), $NiCl_2$ (45 g L^{-1}), H_3BO_3 (35 g L^{-1}) and $C_7H_5NO_3S$ (saccharin, 2.4 g L^{-1}). This electrolyte has a lower Ni^{2+} concentration than conventional Ni electrolyte (Watts bath). The CNT thin film was used as the cathode and a Ni plate (The Nilaco Corp., Tokyo, Japan) was used as the anode. The temperature was maintained at 323 K during the pulsed electrodeposition.

Following the pulsed current electroplating, the MWCNTs/Ni nanocomposite thin film was washed in distilled water several times and dried in air. This operation involving electrodeposition, washing with water and drying in air was repeated three times on the identical sample. The sample was then annealed in air at 523 K for 1 h to oxidize the electrodeposited Ni and also to dehydrate Ni hydroxides, finally to obtain the MWCNTs/NiO nanocomposite thin film.

Cyclic voltammetry (CV) and chronopotentiometry (CP) were carried out using a potentiostat (HZ-5000; Hokuto Denko Corp., Tokyo, Japan) and charge-discharge tester (ECAD-1000; EC Frontier Corp., Kyoto, Japan), respectively. A typical three-electrode

electrochemical cell with a Pt black counter electrode, a saturated calomel electrode (SCE) reference electrode and the CNT/Ni-species nanocomposite electrode was used as the working electrode. The electrolyte was an aqueous KOH solution (6 mol L^{-1}). CV was performed at 1, 10, 30 and 100 mV s^{-1} in a potential window from 0.05 to 0.35 V (vs. SCE). CP was performed at 0.5 A g^{-1} and 7.5 A g^{-1} in a potential window from 0 to 0.30 V (vs. SCE). Before the capacitance measurements, the mass of the MWCNT/NiO nanocomposite electrode was measured using an electronic balance (AUW-220D; Shimadzu Corp., Japan). After the capacitance measurements, the composite layer (exposed to the electrolyte) was manually detached from the SUS316 substrate and the mass of the electrode without the composite was measured. The difference between the mass values of the sample before and after detaching was adopted as the real mass of the deposited nanocomposites.

The samples were observed using a scanning electron microscope (SEM, SU-6600; Hitachi High-Technologies Corporation, Tokyo, Japan) equipped with an energy-dispersive X-ray spectrometer and aberration-corrected, high-resolution transmission electron microscope (JEM-2200FS; JEOL, Tokyo, Japan) equipped with an electron-energy loss spectrometer with energy resolution of 0.8 eV. Energy-dispersive X-ray spectroscopy (EDXS) in the SEM observations was used to acquire the elemental

composition of the nanocomposite sample.

3. Results and discussion

As a result, NiO particles less than 4 nm were deposited on the surface of the MWCNTs (Fig. 1a), unlike the MWCNT before EPD and annealing (Fig. S1 in Supplementary Material). The high-resolution transmission electron microscopy (HR-TEM) images revealed that the lattice fringe of the graphitic multiwall was parallel to the longitudinal direction of the CNTs. The deposited particles had a lattice spacing that was clearly different from that of the graphitic layer spacing (Fig. 1b) and a lattice fringe that was not parallel to the graphitic lattice fringe of the CNTs (Fig. 1c). The fast Fourier transformation of the lattice images of particles revealed that the lattice spacings of the particles coincide with those of NiO (111) and (200). Electron energy loss spectroscopy also revealed the presence of Ni, O and C. The average particle size of NiO particles was calculated to be 3.6 nm according to HR-TEM images (see Fig. S2 in Supplementary Material), although accurate determination of size was difficult due to overlap of particles and lattice fringe of CNTs. EDXS in the SEM observation revealed that the content of NiO in the nanocomposite was 38 ± 2 mass%.

Our previous study has shown that pulsed current electroplating and subsequent

annealing are efficient for the deposition of Ni oxide species particles on MWCNTs; however, the minimum size of the deposited particle was 7 nm [26]. Our present results show that a simple modification of the Watts bath leads to deposition of much finer particles because of the lower Ni^{2+} concentration.

To elucidate the pseudocapacitive behaviour of the MWCNT/NiO nanocomposite electrode, cyclic voltammetry (CV) and chronopotentiometry (CP) were performed with a typical three-electrode electrochemical cell with saturated calomel electrode as a reference electrode, Pt wire as a counter electrode and the nanocomposite electrode as a working electrode. The electrolyte was 6 mol L^{-1} KOH aqueous solution. CV curves at different scan rates of 1–100 mV s^{-1} are shown in Fig. 2a. The magnitude of the current increased with the scan rate. A pair of redox peaks with a midpoint potential of 0.17 V (vs. saturated calomel electrode) were detected, which is attributed to the redox reaction of NiO/NiOOH, similar to previous studies [26].

The specific capacitance (C) per mass of MWCNT/NiO nanocomposite thin film was determined from the CV curves using the following equation [7,12]:

$$C = \frac{1}{2mv\Delta V}\int_{V_i}^{V_f} |I|\, dV,$$

where m is the mass of the MWCNTs/NiO composite, ΔV is the potential window, V_i and V_f are the initial and final potentials in one cycle, respectively, I is the

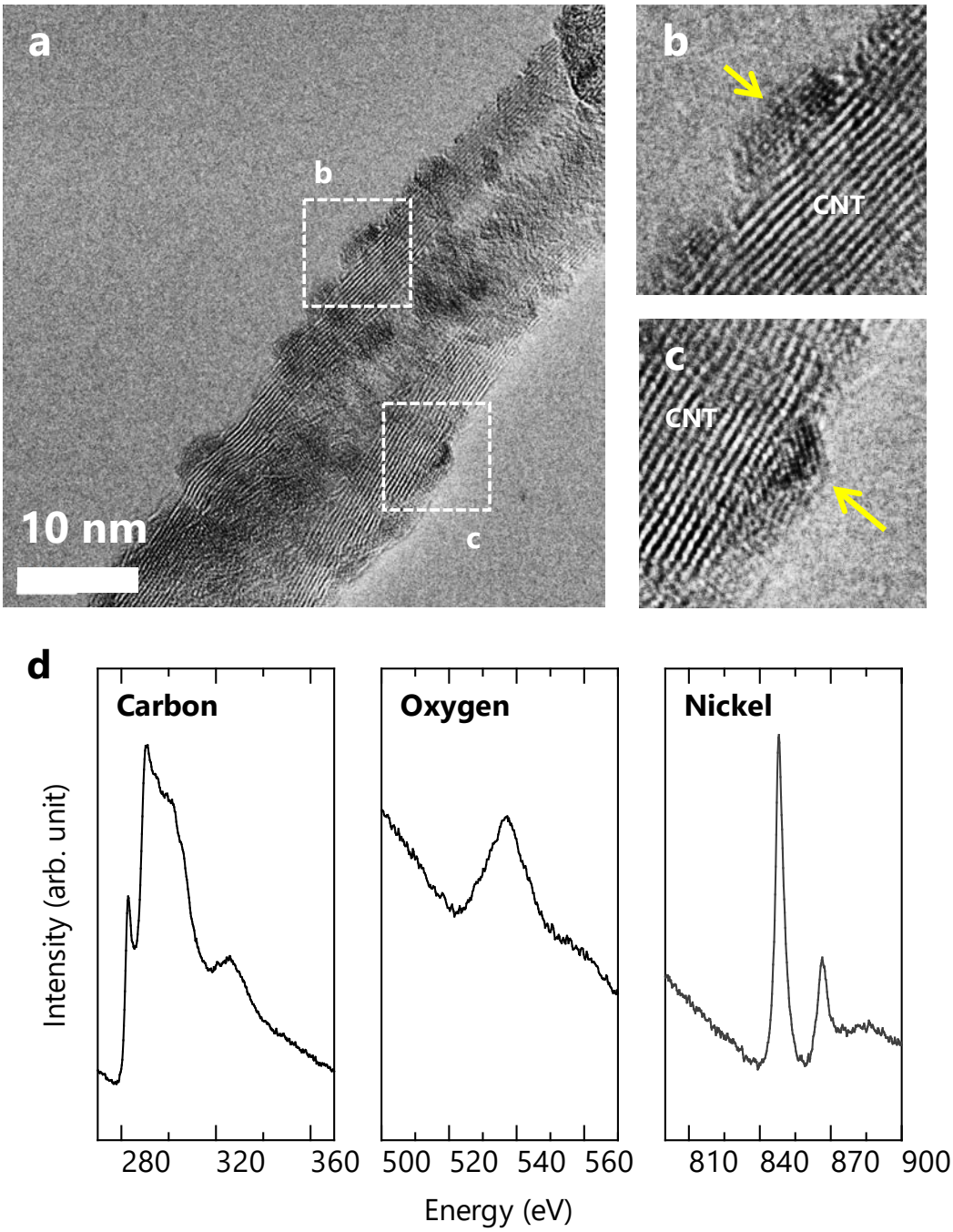

Fig. 1 (a) High-resolution transmission electron microscopy (HR-TEM) image of MWCNTs/NiO nanocomposites fabricated by pulsed current electroplating in a modified Watts bath. (b and c) Enlarged images of (a), showing the lattice fringes of the deposited particles (arrows) whose crystal lattices are different from those of the graphitic lattice of the CNT. (d) Electron energy loss spectroscopy profile of MWCNTs/NiO nanocomposites fabricated by pulsed current electroplating in a modified Watts bath. Nickel, oxygen and carbon were detected.

instantaneous current at a given potential and v is the scan rate. The calculated specific capacitances per mass of MWCNTs/Ni-species nanocomposite electrode at the scan rates of 1, 10, 30 and 100 mV s^{-1} are 1505, 1208, 807 and 570 F g^{-1}, respectively. The capacitances per mass of NiO, which can be calculated from the results of the energy-dispersive X-ray spectroscopy of the sample, were 2253, 1808, 1203 and 853 F g_{NiO}^{-1}, respectively.

Fig. 2b shows the galvanostatic discharge curves at different discharge currents from the MWCNTs/NiO nanocomposite electrode. The potential decreased monotonically with time and a higher current provided a shorter discharge time, which is a similar trend to the discharge tests of metal oxide-based pseudocapacitors [26].

The capacitances of the MWCNTs/NiO nanocomposite electrode were also calculated from the discharge curves using the following equation [11]:

$$C = \frac{I\Delta t}{m\Delta V},$$

where I is the discharge current, m is the mass of MWCNTs/NiO nanocomposite, Δt is the discharge time and ΔV is the potential window. At I/m (discharge current per mass of sample) of 0.5 and 7.5 A g_{NiO}^{-1}, calculated capacitances per mass of MWCNTs/NiO nanocomposite were 1657 and 1175 F g^{-1}, respectively. Specific capacitances per mass of NiO are calculated to be 2480 and 1759 F g_{NiO}^{-1} at each

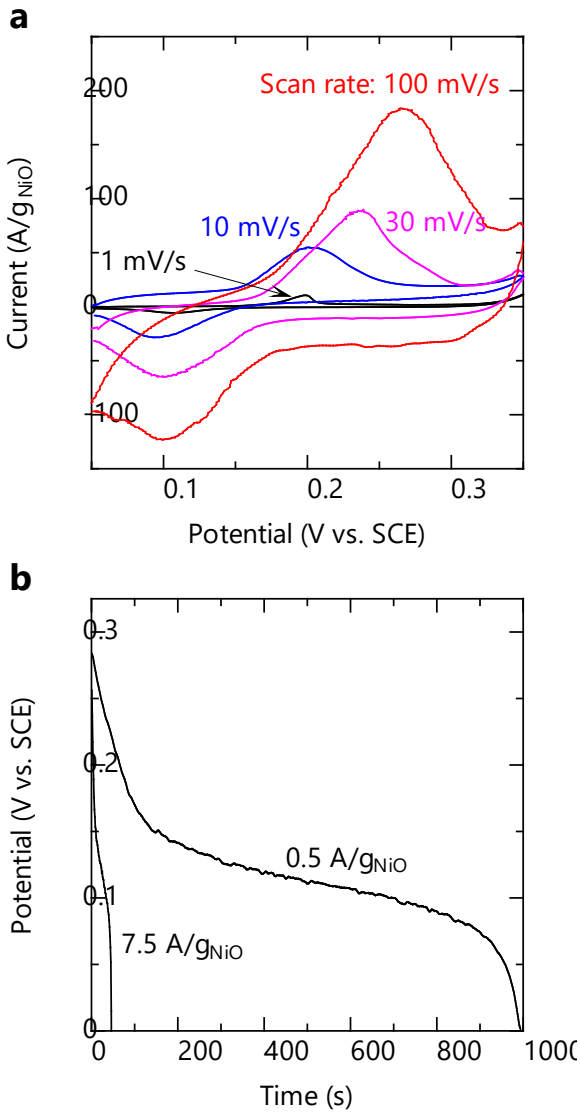

Fig. 2 (a) Cyclic voltammetry (CV) and (b) chronopotentiometry (CP) curves of MWCNTs/Ni-species nanocomposites fabricated by pulsed current electroplating in a modified Watts bath. A typical three-electrode electrochemical cell and an electrolyte of 6 mol L^{-1} KOH aqueous solution were used with the fabricated nanocomposite electrode as the working electrode.

discharge current..

Comparison between the capacitance per mass of the active Ni species of the present MWCNTs/NiO nanocomposite electrode and previous results [3–9,11,13–

16,26,28] is shown in Fig. 3. As shown in Fig. 3a, the capacitances of the present nanocomposite electrodes evaluated by CV are higher than the capacitances of previous studies for most of the Ni-species pseudocapacitive electrodes at every scan rate. In particular, at low scan rates, the capacitance of the present nanocomposite electrode is much higher than the others. Similarly, the capacitances of the present nanocomposite electrode evaluated by CP measurements are higher than those in previous studies, as shown in Fig. 3b. The theoretical capacitances of NiO are 2584 F g^{-1} within a potential width of 0.5 V [7,16]. Therefore, the present MWCNTs/NiO nanocomposites provide a capacitance very close to the theoretical values.

Energy density (E) and power density (P) can be calculated by the following equations [29,30]:

$$E = \frac{1}{2} C \Delta V^2$$

$$P = \frac{E}{\Delta t}$$

At I/m of 0.5 and 7.5 A g_{NiO}^{-1}, E were calculated to be 21 and 15 Wh kg^{-1}, while P were 0.08 and 1.1 kW kg^{-1}, respectively. Although these values of density were not always as high as those in literatures [10,28] perhaps due to narrow potential window, there is much room for further investigation.

The Faradaic reactions of NiO are described by the following equation [31]:

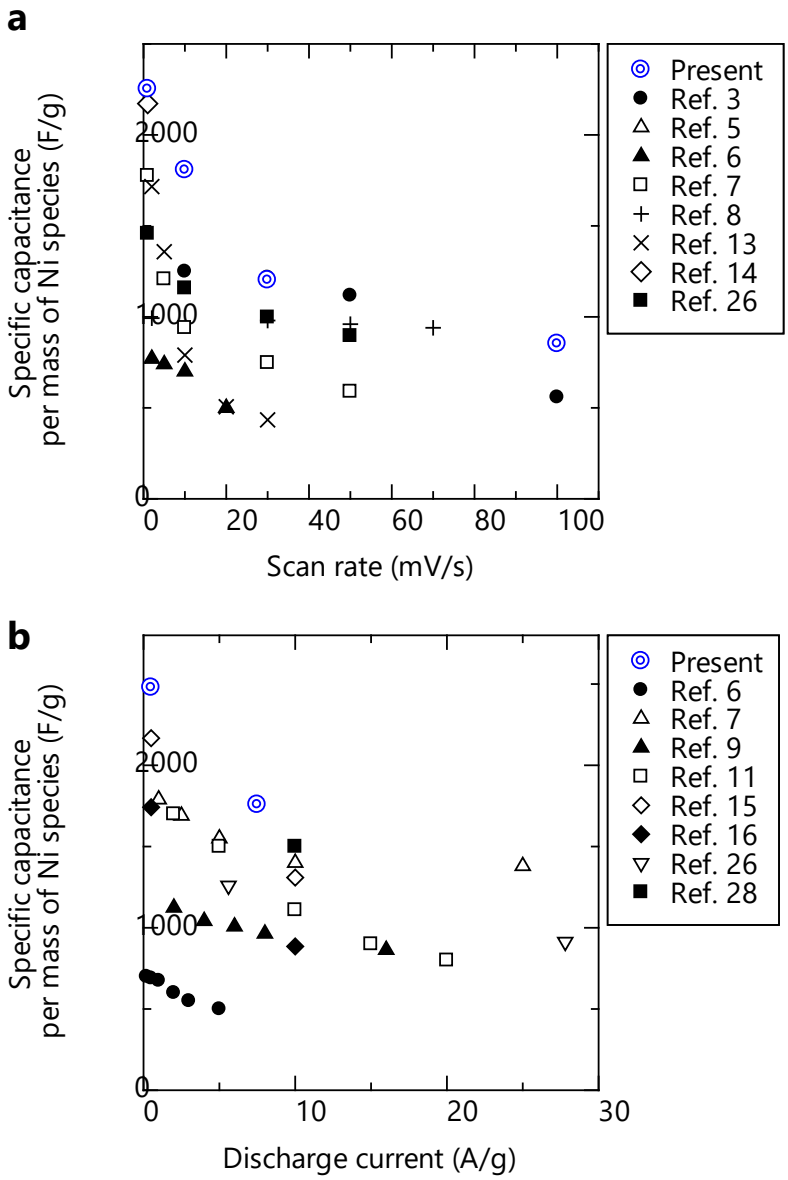

Fig. 3 Comparison of the capacitances between the present MWCNTs/Ni-species nanocomposite electrode and other Ni-species nanostructured pseudocapacitive electrodes. Capacitances are evaluated by (a) CV and (b) CP measurements.

$$NiO + OH^- \leftrightarrow NiOOH + e^-.$$

The redox reactions occur at the interface between the electrolyte and the NiO

nanoparticles. To increase the effective specific capacitance of the active NiO, the specific surface area of the NiO particles should be increased. In the present study, reduction of the size of the deposited Ni particles led to an increase in the specific surface area, which consequently provides more reaction sites for the redox reactions in the composite electrode.

To the best of our knowledge, the deposited Ni oxide particles used in the present nanocomposite electrode are the smallest (4 nm) of those reported. In our previous study, we reported the pseudocapacitance of similar MWCNTs/Ni-species nanocomposite electrodes prepared from particles with a diameter of 7 nm, where the conventional Watts bath was used for Ni pulsed current electroplating [26]. Assuming that the deposited particles are hemispherical, the specific surface area of NiO is proportional to the reciprocal of the diameter. Hence, the reduction of size from 7 to 4 nm means there is 1.75 times increase of the specific surface area, which roughly corresponds to the multiplying factor of 1.56 of the corresponding capacitances obtained at low scan rates. This correlation indicates that the high capacitance of the present nanocomposite electrode can be mainly attributed to the higher specific surface area where the redox reactions occur. The extraordinarily small size of the active NiO results from the low concentration of Ni^{2+} used in the modified Watts bath, which successfully suppresses the

grain growth.

4. Conclusions

The modified Watts bath coupled with pulsed current electroplating led to the fabrication of MWCNTs/NiO pseudocapacitive electrodes with extraordinarily small active NiO particles. HR-TEM observations (Fig. 1) revealed very fine NiO particles with a size of less than 4 nm on the surface of the CNT in the nanocomposite electrodes. The smaller size of the deposited Ni oxide particles provides a larger interface between the deposited NiO nanoparticles and the electrolyte. As a result of uniform dispersion of the ultrafine NiO particles on the MWCNTs, the nanocomposite electrodes have distinguished capacitances.

Acknowledments

HR-TEM observations with electron energy loss spectroscopy analyses were technically supported by Kyoto University Nano Technology Hub in the “Nanotechnology Platform Project” sponsored by the Ministry of Education, Culture, Sports, Science and Technology, Japan. Observations by scanning electron microscopy were conducted in the Research and Education Center of Advanced Energy Science, Graduate School of Energy

Science, Kyoto University.

Appendix A. Supplementary Material

Supplementary Material associated with this article can be found in the online version at doi: [to be inserted].

References

[1] C.-T. Hsieh, Y.-W. Chou, W.-Y. Chen, Synthesis and electrochemical characterization of carbon nanotubes decorated with nickel nanoparticles for use as an electrochemical capacitor, J. Solid State Electrochem. 12 (2008) 663–669.

[2] B. Gao, C.-Z. Yuan, L.-H. Su, L. Chen, X.-G. Zhang, Nickel oxide coated on ultrasonically pretreated carbon nanotubes for supercapacitor, J. Solid State Electrochem. 13 (2009) 1251–1257.

[3] B. Wen, S. Zhang, H. Fang, W. Liu, Z. Du, Electrochemically dispersed nickel oxide nanoparticles on multi-walled carbon nanotubes, Mater. Chem. Phys. 131 (2011) 8–11.

[4] J.Y. Lee, K. Liang, K.H. An, Y. H. Lee, Nickel oxide/carbon nanotubes nanocomposite for electrochemical capacitance, Synth. Met. 150 (2005) 153–157.

[5] K.-W. Nam, K.-H. Kim, E.-S. Lee, W.-S. Yoon, X.-Q. Yang, K.-B. Kim, Pseudocapacitive properties of electrochemically prepared nickel oxides on 3-dimensional carbon nanotube film substrates, J. Power Sources 182 (2008) 642–652.

[6] X. Zhu, H. Dai, J. Hu, L. Ding, L. Jiang, Reduced graphene oxide–nickel oxide composite as high performance electrode materials for supercapacitors, J. Power Sources 203 (2012) 243–249.

[7] K. Liang, X. Tang, W. Hu, High-performance three-dimensional nanoporous NiO film

as a supercapacitor electrode, J. Mater. Chem. 22 (2012) 11062–11067.

[8] K.-W. Nam, E.-S. Lee, J.-H. Kim, Y.-H. Lee, K.-B. Kim, Synthesis and Electrochemical Investigations of $Ni_{1-x}O$ Thin Films and $Ni_{1-x}O$ on Three-Dimensional Carbon Substrates for Electrochemical Capacitors, J. Electrochem. Soc. 152 (2005) A2123–A2129.

[9] C. Yuan, J. Li, L. Hou, L. Yang, L. Shen, X. Zhang, Facile growth of hexagonal NiO nanoplatelet arrays assembled by mesoporous nanosheets on Ni foam towards high-performance electrochemical capacitors, Electrochim. Acta 78 (2012) 532–538.

[10] Q. Lu, M.W. Lattanzi, Y. Chen, X. Kou, W. Li, X. Fan, K. M. Unruh, J. G. Chen, J. Q. Xiao, Supercapacitor Electrodes with High-Energy and Power Densities Prepared from Monolithic NiO/Ni Nanocomposites, Angew. Chem. Int. Ed. 50 (2011) 6847–6850.

[11] M. Yang, J. X. Li, H.H. Li, L.W. Su, J.P. Wei, Z. Zhou, Mesoporous slit-structured NiO for high-performance pseudocapacitors, Phys. Chem. Chem. Phys. 14 (2012) 11048–11052.

[12] K.-W. Nam, K.-B. Kim, A Study of the Preparation of NiO_x Electrode via Electrochemical Route for Supercapacitor Applications and Their Charge Storage Mechanism, J. Electrochem. Soc. 149 (2002) A346–A354.

[13] H. Cheng, K.L.P. Koh, P. Liu, T.Q. Thang, H.M. Duong, Continuous self-assembly

of carbon nanotube thin films and their composites for supercapacitors, Colloids Surf. A: Physicochem. Eng. Aspects 481 (2015) 626–632.

[14] F. Gu , X. Cheng , S. Wang , X. Wang, P.S. Lee, Oxidative Intercalation for Monometallic Ni^{2+}-Ni^{3+} Layered Double Hydroxide and Enhanced Capacitance in Exfoliated Nanosheets, Small 11 (2015) 2044–2050.

[15] H. Chen, Y. Kang, F. Cai, S. Zeng, W. Li, M.C.Q. Li, Electrochemical conversion of $Ni_2(OH)_2CO_3$ into $Ni(OH)_2$ hierarchical nanostructures loaded on a carbon nanotube paper with high electrochemical energy storage performance, J. Mater. Chem. A 3 (2015) 1875–1878.

[16] L. Wang, H. Chen, F. Cai. M. Chen, Hierarchical carbon nanotube/α-$Ni(OH)_2$ nanosheet composite paper with enhanced electrochemical capacitance, Mater. Lett. 115 (2014) 168–171.

[17] S.-M. Bak, K.-H. Kim, C.-W. Lee, K.-B. Kim, Mesoporous nickel/carbon nanotube hybrid material prepared by electroless deposition, J. Mater. Chem. 21 (2011) 1984–1990.

[18] K.-Y. Lin, W.-T. Tsai, J.-K. Chang, Decorating carbon nanotubes with Ni particles using an electroless deposition technique for hydrogen storage applications, Int. J. Hydrogen Energy 35 (2010) 7555–7562.

[19] C.-Y. Chen, K.-Y. Lin, W.-T. Tsai, J.-K. Chang, C.-M. Tseng, Electroless deposition

of Ni nanoparticles on carbon nanotubes with the aid of supercritical CO_2 fluid and a synergistic hydrogen storage property of the composite, Int. J. Hydrogen Energy 35 (2010) 5490–5497.

[20] Z. Liu, Z. Li, F. Wang, J. Liu, J. Ji, K. C. Park, M. Endo, Electroless preparation and characterization of Ni–B nanoparticles supported on multi-walled carbon nanotubes and their catalytic activity towards hydrogenation of styrene, Mater. Res. Bull. 47 (2012) 338–343.

[21] Y.I. Golovin, D.Y. Golovin, A.V. Shuklinov, R.A. Stolyarov, V.M. Vasyukov, Electrodeposition of Nickel Nanoparticles onto Multiwalled Carbon Nanotubes, Tech. Phys. Lett. 37 (2011) 253–255.

[22] N. Chopra, W. Shi, A. Bansal, Structural evolution and stability studies of heterostructures comprised of carbon nanotubes decorated with nickel/nickel oxide core/shell nanoparticles, Carbon 49 (2011) 3645–3662.

[23] N. Chopra, H. G. McWhinney, W. Shi, Chemical changes in carbon Nanotube-Nickel/Nickel Oxide Core/Shell nanoparticle heterostructures treated at high temperatures, Mater. Charact. 62 (2011) 635–641.

[24] H. Natter, R. Hempelmann, Tailor-made nanomaterials designed by electrochemical methods, Electrochim. Acta 49 (2003) 51–61.

[25] H. Natter, M. Schmelzer, R. Hempelmann, Nanocrystalline nickel and nickel-copper alloys: Synthesis, characterization, and thermal stability, J. Mater. Res. 13 (1998) 1186–1197.

[26] M. Hakamada, A. Moriguchi, M. Mabuchi, Fabrication of carbon nanotube/$NiO_x(OH)_y$ nanocomposite by pulsed electrodeposition for supercapacitor applications, J. Power Sources 245 (2014) 324–330.

[27] D. Bom, R. Andrews, D. Jacques, J. Anthony, B. Chen, M. S. Meier, J. P. Selegue, Thermogravimetric analysis of the oxidation of multiwalled carbon nanotubes: evidence for the role of defect sites in carbon nanotube chemistry, Nano Lett. 2002, 2, 615–619.

[28] D.-S. Kong, J.-M. Wang, H.-B. Shao, J.-Q. Zhang, C.-N. Cao, Electrochemical fabrication of a porous nanostructured nickel hydroxide film electrode with superior pseudocapacitive performance, J. Alloy. Compd. 2011, 509, 5611–5616.

[29] M. Zhi, C. Xiang, J. Li, M. Li, N. Wu, Nanostructured carbon-metal oxide composite electrodes for supercapacitors: a review, Nanoscale 2013, 5, 72–88.

[30] A. Zolfaghari, F. Ataherian, M. Ghaemi, A. Gholami, Capacitive behavior of nanostructured MnO_2 prepared by sonochemistry method, Electrochim. Acta 2007, 52, 2806–2814.

[31] M. S. Wu, H. H. Hsieh, Nickel oxide/hydroxide nanoplatelets synthesized by

chemical precipitation for electrochemical capacitors, Electrochim. Acta 53 (2008) 3427–3435.

Figure captions

Fig. 1 (a) High-resolution transmission electron microscopy (HR-TEM) image of MWCNTs/NiO nanocomposites fabricated by pulsed current electroplating in a modified Watts bath. (b and c) Enlarged images of (a), showing the lattice fringes of the deposited particles (arrows) whose crystal lattices are different from those of the graphitic lattice of the CNT. (d) Electron energy loss spectroscopy profile of MWCNTs/NiO nanocomposites fabricated by pulsed current electroplating in a modified Watts bath. Nickel, oxygen and carbon were detected.

Fig. 2 (a) Cyclic voltammetry (CV) and (b) chronopotentiometry (CP) curves of MWCNTs/Ni-species nanocomposites fabricated by pulsed current electroplating in a modified Watts bath. A typical three-electrode electrochemical cell and an electrolyte of 6 mol L^{-1} KOH aqueous solution were used with the fabricated nanocomposite electrode as the working electrode.

Fig. 3 Comparison of the capacitances between the present MWCNTs/Ni-species nanocomposite electrode and other Ni-species nanostructured pseudocapacitive electrodes. Capacitances are evaluated by (a) CV and (b) CP measurements.

Electrodes from carbon nanotubes/NiO nanocomposites synthesized in modified Watts bath for supercapacitors

Masataka Hakamada*, Tatsuhiko Abe, Mamoru Mabuchi

Department of Energy Science and Technology, Graduate School of Energy Science, Kyoto University, Yoshidahonmachi, Kyoto, 606-8501 Japan

*Corresponding author. E-mail: hakamada.masataka.3x@kyoto-u.ac.jp (M. Hakamada).

1. Characterization of multiwalled carbon nanotubes (MWCNTs)

Figure S1a and S1b shows the high-resolution transmission electron microscopy (HR-TEM) images of MWCNTs after the electrophoretic deposition (EPD) on SUS316L substrate and subsequent insulation annealing (before pulsed current electroplating of Ni). The lattice fringe of the graphitic multiwall was parallel to the longitudinal direction of the CNTs. Although lattice disorder, which may be due to the acid treatment before EPD, has been observed at the limited portion of the surface of nanotubes, the CNTs shows typical characteristics of MWCNTs. Electron-energy loss spectrometer with energy resolution of 0.8 eV (Fig. S1c) detected large portion of carbon and small amount of oxygen. The oxygen seems to be introduced during the acid treatment for EPD.

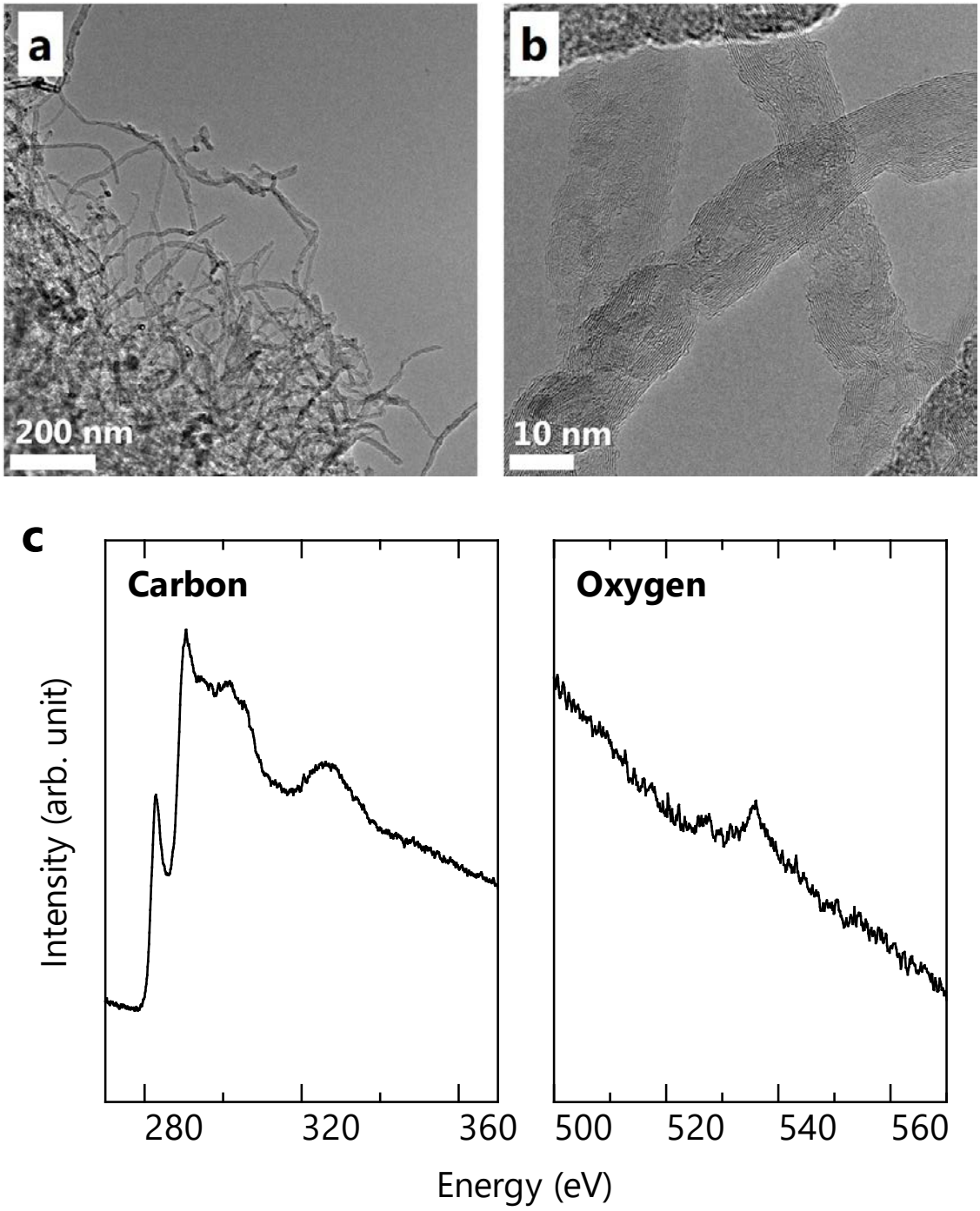

Fig. 1 (a and b) Transmission electron microscopy (HR-TEM) image of MWCNTs. (c) Electron energy loss spectroscopy profile of MWCNTs.

2. Size distribution of NiO particles

Figure S2 shows the histogram of the size of NiO particles deposited on MWCNTs, where HR-TEM images were used. The average size of NiO particles was 3.6 nm, although accurate determination was difficult due to overlap of particles and lattice fringe of CNTs.

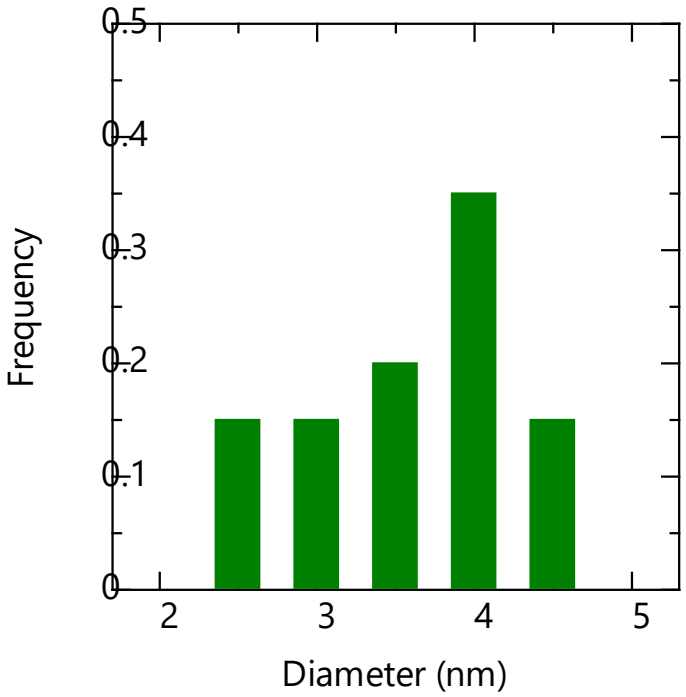

Fig. 2 Histogram of diameter of NiO particles deposited on MWCNTs, where HR-TEM images were used.